Controlling high harmonic generation with molecular wave packets

Itatani, J.; Zeidler, D.; Levesque, J.; Spanner, M.; Villeneuve, D. M.; Corkum, P. B.

Publisher's version / Version de l'éditeur:
https://doi.org/10.1103/PhysRevLett.94.123902
Physical Review Letters, 94, 12, 2005-03-31

Controlling High Harmonic Generation with Molecular Wave Packets

J. Itatani,[1,2,*] D. Zeidler,[1] J. Levesque,[1,3] Michael Spanner,[1,4] D. M. Villeneuve,[1] and P. B. Corkum[1]

[1]*National Research Council Canada, Ottawa, Ontario, K1A 0R6 Canada*
[2]*University of Ottawa, 150 Louis Pasteur, Ottawa, Ontario, K1N 6N5 Canada*
[3]*INRS Énergie, Matériaux et Télécommunications, Varennes, Québec, J3X 1S2 Canada*
[4]*Department of Physics, University of Waterloo, Ontario, N2L 3G1 Canada*

(Received 12 June 2004; published 31 March 2005)

We show that, by controlling the alignment of molecules, we can influence the high harmonic generation process. We observed strong intensity modulation and spectral shaping of high harmonics produced with a rotational wave packet in a low-density gas of N_2 or O_2. In N_2, where the highest occupied molecular orbital (HOMO) has σ_g symmetry, the maximum signal occurs when the molecules are aligned along the laser polarization while the minimum occurs when it is perpendicular. In O_2, where the HOMO has π_g symmetry, the harmonics are enhanced when the molecules are aligned around 45° to the laser polarization. The symmetry of the molecular orbital can be read by harmonics. Molecular wave packets offer a means of shaping attosecond pulses.

DOI: 10.1103/PhysRevLett.94.123902 PACS numbers: 42.65.Ky, 33.80.Rv, 33.15.Mt, 39.90.+d

Underlying much of strong-field atomic and molecular physics is a fast-moving electron produced by field ionization of an atom or molecule, accelerated in the laser field and recolliding with its parent ion with subfemtosecond precision [1]. High harmonic and attosecond pulse generation requires the coherent interaction between this electron and an emitted photon in the presence of the parent atom or molecule. All three parts—electrons, photons, and atoms or molecules offer opportunities to attosecond science. Electrons can probe molecular structure [2,3] and the structure can be read by the harmonics that are produced [4,5]. Once the relation between molecular structures and harmonics is understood [5], it should become possible to control *molecules* to shape harmonics, sculpt attosecond pulses, and increase harmonic generation efficiency.

Shortly after their origin was understood in atomic systems, high harmonics were produced in molecular media. These experiments showed that randomly aligned ensembles behave in a qualitatively similar manner to atomic media [6,7]. However, recent experiments on randomly aligned molecules indicate that, depending on the molecular orbital symmetry, the behavior of harmonics cutoff differs from atoms [8]. Theoretical studies further predict that the strength and phase of harmonics should depend on molecular structure and its alignment [4,5].

There are two ways to align molecular ensembles—adiabatically [9] and nonadiabatically [10]. Experiments on adiabatically aligned molecules show a weak effect of alignment and orbital symmetry on harmonic yields [11,12]. We use nonadiabatic alignment where two recent publications have reported that the harmonic strength is more strongly modulated [13,14].

We build on these experiments. Producing harmonics from rotational wave packets in N_2 molecules, we observed a contrast ratio of 10.6:1 for the 23rd harmonic between molecules parallel and perpendicular to the polarization of the fundamental laser pulse. Smaller, but still large contrast ratios are measured for all harmonics, even for those in the cutoff region. Such large control over the whole harmonics opens a new route to quasi-phase-matching.

We also measure the ellipticity dependence of the harmonic strength as a function of alignment for both N_2 and O_2. This allows us to identify that the last step of the 3-step process responsible for high harmonic generation (HHG) [1]—recollision—is the most sensitive to alignment. Thus, the rotational wave packet structure is mapped in a simple way onto the *spectrum, phase, and polarization* of high harmonics or attosecond pulses.

The highest occupied molecular orbital (HOMO) in O_2 has different symmetry from N_2. Using O_2, we clearly confirm that the symmetry of HOMO is important for the harmonic emission. We show that the harmonic emission peaks for molecules aligned near 45° with respect to laser polarization, but not exactly at 45°.

For our measurements, we used a pulsed gas jet with a width of ~ 1 mm, a density of $\sim 10^{17}/\mathrm{cm}^3$, and a rotational temperature of ~ 30 K, in the interaction region. The output from a Ti:sapphire chirped-pulsed amplifier that is capable of producing 1-TW 30-fs pulses at 50 Hz, is divided into pump and probe pulses with a Mach-Zender interferometer inserted before the pulse compressor. The two laser beams propagate collinearly and were loosely focused about 1 mm below the orifice (100 μm diameter) of the gas jet. The confocal parameters of the focused beams were longer than the gas jet size, and the foci were placed before the jet.

We used a 60-fs, 800-nm pump pulse to produce a rotational wave packet in N_2 or O_2. The beam size of this pulse was set by an aperture in the interferometer to have a focused spot size larger than the probe. The intensity at the focus was $\sim 4 \times 10^{13}$ W/cm^2 where no ions are de-

tected by a dc-biased electrode placed near the gas jet and no harmonic emission was measured from this pump alone.

After a fixed time delay, an intense 35-fs probe pulse is focused into the gas jet with $f^{\#} \sim 50$. An aperture near the focusing lens is used to optimize the harmonic intensities. The polarization of the probe pulse is the same as the pump and the intensity was estimated to be $\sim 2 \times 10^{14}$ W/cm^2 from the high harmonic cutoff. This laser intensity is well below the saturation intensity, ensuring that high harmonics are emitted at the peak of the laser pulse. Under our experimental condition, the geometrical phase shift dominates the phase mismatch, reducing the intensity of higher orders. However, its influence on the harmonic spectrum can be cancelled by normalizing the harmonic signal against the randomly aligned case.

The harmonics were measured by an extreme UV (XUV) spectrometer in a second differentially pumped chamber. Both the laser and XUV beams passed through a narrow spectrometer slit. An aberration-corrected concave grating spectrally dispersed the harmonics and relayed the spectral image onto the MgF-coated microchannel plates backed by a phosphor screen. A charge-coupled device camera outside the chamber accumulated the spectral image for 500 shots.

The time evolution of a rotational wave packet simulated under similar conditions to our experiment with an initial rotational temperature of 30 K is represented in Fig. 1 (dotted black curve, right axis) for N_2. In the figure, the right vertical axis plots the degree of alignment given by $\langle \cos^2\theta \rangle$, where θ is the angle between the laser polarization and the internuclear axis, and $\langle\rangle$ denotes the ensemble average. A large value of $\langle \cos^2\theta \rangle$ corresponds to alignment along the direction of the laser polarization. A small value corresponds to alignment perpendicular; $\langle \cos^2\theta \rangle = 1/3$ for an isotropic distribution.

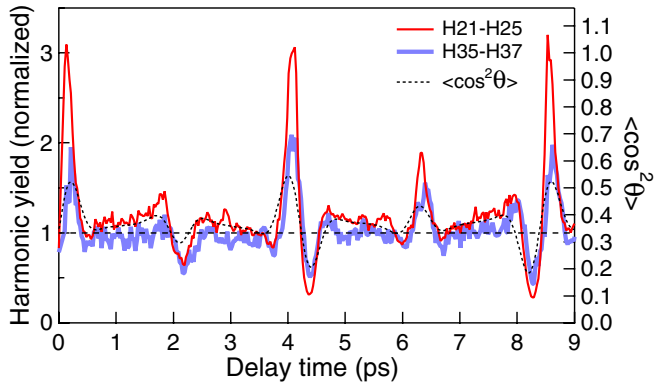

FIG. 1 (color online). Temporal evolution of the rotational wave packet in N_2. Right axis: simulated $\langle \cos^2\theta \rangle$ of the angular distribution of the molecular axis (dotted black curve). Left axis: normalized magnitudes of the observed high harmonic signals, integrated over the harmonics 21st-25th (thin red curve) and over the 35th-37th (thick blue curve). The common horizontal dashed line shows the normalized harmonic intensity (= 1, left axis) and $\langle \cos^2\theta \rangle$(= 1/3, right axis) for the randomly aligned case.

Figure 1 also plots the intensities of the harmonic signal integrated over the 21st to 25th (plateau region, thin red curve, left axis) and over the 35th to 37th (cutoff region, thick blue curve, left axis) normalized against the randomly aligned case [15]. The maximum signal contrast between parallel and perpendicular alignment reaches ~10.6:1 for the 23rd harmonic in the plateau region. We observed that all the harmonics show similar revival structures with the same time scale. We thus conclude that harmonic emission is enhanced when the N_2 molecules are aligned parallel to the laser field and suppressed when the molecules are perpendicular. In addition, we observed that the cutoff order of harmonics remains the same at all the delay times. This fact suggests that the alignment dependence of ionization probability does not play a significant role in the observed modulation of harmonic yields. Clearly, the high contrast of harmonic yields that we observed show that molecular alignment will allow quasi-phase-matching. By spatially modulating the molecular alignment along the path of the fundamental laser pulse instead of controlling the pulse itself [16,17], the nonlinearity can be turned on and off to increase the phase-matched interaction length.

Next we concentrate on the physical mechanism responsible for the strong alignment dependence of HHG. Each step in the 3-step quasistatic model [1]—(1) tunnel ionization, (2) propagation of an electron wave packet in the continuum, and (3) recollision with the atom or molecule from which the wave packet originated—has a potential to influence the alignment dependence of the harmonic signal. The tunnelling rate must be alignment dependent [18,19] because of the variation of the wave function near the saddle-point region where the electron tunnels out. Potentially, this dependence of tunnelling is important because the harmonic signal is directly proportional to the ionization rate. However, maximum alignment achieved in our rotational wave packets is modest [18]. The maximum contrast of the ionization rate as a function of alignment was measured to be ~25% for N_2, and less (but below experimental error) for O_2 [18]. Thus the alignment dependence of the ionization rate only plays a small role.

The wave packet propagation in the continuum is also alignment dependent because the tunneling ionization determines the initial condition of the wave packet. The lateral width of the saddle-point region through which the electron must tunnel determines the lateral velocity that the electron acquires on tunnelling. The larger the lateral velocity spread is, the weaker the amplitude of the recolliding wave packet. The strength of the harmonic signal is proportional to the recollision probability. We measured the lateral spread of the wave packet at the time of recollision through the ellipticity dependence of the harmonic signal [20]. For N_2 and O_2, the alignment

dependence of the lateral spread is small but easily observable. Under our experimental condition with N_2, the alignment dependence of the tunnelling and the wave packet spread almost cancel each other. Thus, we conclude that the final step, recollision, plays the dominant role in the alignment dependence of HHG.

Figure 2 illustrates the final step. At the top left, the HOMO of N_2 (σ_g), aligned parallel to the field, is shown. The electron tunnels from this molecular orbital wave function, Ψ_g. The recolliding electron wave packet Ψ_c, shown as a plane wave in the middle, overlaps the remaining portion of the wave function. The coherent addition of the two portions of the same wave function induces a dipole given by $\mathbf{d}(t) = \langle \Psi_g | e\mathbf{r} | \Psi_c \rangle + \text{c.c.}$, which is seen as the asymmetric localization of electron density (the square of superposed wave functions in the middle) at the bottom in Fig. 2(a). The induced dipole oscillates as the continuum electron wave propagates though the molecule. It is this oscillating dipole that emits high harmonic radiation. Both the size of the ground-state wave function and the wavelength of the continuum electron determine the strength of the induced dipole and therefore the spectral intensity of each harmonic. By controlling molecules, we

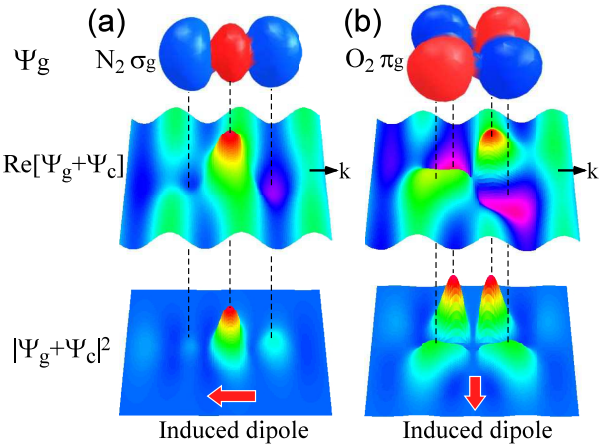

FIG. 2 (color online). The dipole acceleration is responsible for the harmonic signal. We illustrate the physical mechanism responsible for the dipole. The upper panels sketch the HOMO for N_2 σ_g (left) and O_2 π_g (right) aligned parallel to the laser electric field. The color represents the sign of the wave function. The middle panels show the real part of the coherent superposition of the molecular orbital Ψ_g and the recolliding electron wave packet Ψ_c. The continuum electron is propagating in the direction parallel to the field (shown by the arrows denoted by k). The coherent addition of Ψ_g and Ψ_c induces a dipole. The bottom panels show the square of the wave function. The induced dipoles can be seen as the asymmetric localization of the electron densities, while the red (lower) arrows show the directions of the dipoles. For N_2, the dipole oscillates along the electric field direction as the electron propagates, leading to harmonic emission. For O_2, the dipole oscillates in the perpendicular direction, thus harmonic emission is forbidden; see text for explanation.

can change the spatial distribution and the phase of Ψ_g to influence the induced dipole, or to shape the intensity and the chirp of high harmonics.

Figure 2 shows that the molecular orbital of N_2 is larger along the internuclear axis than perpendicular. Thus, for long-wavelength recolliding electrons, the induced dipole is larger for molecules aligned parallel to the direction of electron propagation (and laser polarization).

To illustrate the dependence of the induced dipole on molecular orbital symmetry, we sketch the HOMO of O_2 (π_g) in Fig. 2(b), top panel. The internuclear axis of O_2 is aligned parallel to the propagating direction of the returning electron. For this illustration, we have chosen the electron wavelength to be approximately twice the internuclear separation. The figure illustrates that the induced dipole oscillates in the perpendicular direction to the electron motion because of the shape of the molecular orbital.

Perpendicularly polarized harmonic emission cannot be observed in our experiment because the rotational wave packet has inversion symmetry with respect to the polarization plane of the probe pulse. The symmetry of the wave packet suppresses the constructive interference of perpendicular emission from a large number of molecules. Because of the shape of the molecular orbital, the induced dipole in the directions parallel or perpendicular to the internuclear axis should be very weak. In contrast, if the molecule is aligned at $\sim 45°$ to the laser polarization (not illustrated), a dipole parallel to the field is strongly induced. Thus, enhanced harmonic emission occurs when O_2 is aligned at $\sim 45°$.

In Fig. 3(a), we plot the calculated values of $\langle \cos^2\theta \rangle$ (thick gray curve, left axis) and $\langle \sin^2 2\theta \rangle$ (thin black curve, right axis) for an O_2 rotational wave packet as a function of the pump-probe delay. A large value of $\langle \sin^2 2\theta \rangle$ corresponds to an ensemble of molecules aligned primarily at $45° + n \times 90°$ to the laser polarization. A small value corresponds to molecules primarily aligned at $n \times 90°$. For a randomly aligned ensemble, $\langle \sin^2 2\theta \rangle = 8/15$.

Figure 3(b) (thick red curve, left axis) shows the harmonic intensities integrated over the 17th to 35th observed under similar condition to N_2 [21]. For convenience we reproduce $\langle \sin^2 2\theta \rangle$ (thin black curve, right axis) from Fig. 3(a). The change of harmonic intensities approximately matches $\langle \sin^2 2\theta \rangle$, but is not at all like $\langle \cos^2\theta \rangle$. For example, the revival structure of harmonics near 4.3 ps has no counterpart in the $\langle \cos^2\theta \rangle$ distribution. However, there are small timing differences (up to 0.2 ps) between the revivals of $\langle \sin^2 2\theta \rangle$ and the harmonic signal. We conclude that it is because the HOMO of O_2 does not exactly have fourfold symmetry. Therefore, the harmonic signal from O_2 maximizes near, but not exactly at, $\theta = 45°$. Because of the exact twofold symmetry of the molecular orbital, the harmonic signal is minimum when the molecular ensemble is exactly parallel or perpendicular to the laser polarization.

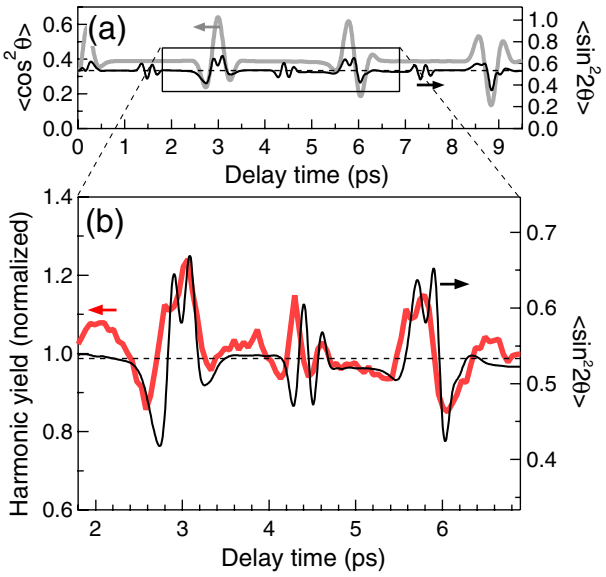

FIG. 3 (color online). Temporal evolution of a rotational wave packet in O_2. (a) Two different representations of the rotational wave packet: $\langle\cos^2\theta\rangle$ (thick gray curve, left axis); $\langle\sin^2 2\theta\rangle$ (thin black curve, right axis). The common horizontal dotted line shows the values for the randomly aligned case. (b) Right axis: $\langle\sin^2 2\theta\rangle$ (thin black curve) as shown in the gray square area of (a). Left axis: normalized magnitude of the spectrally-integrated harmonic signal (thick red curve). The common horizontal dashed line shows the values for the randomly aligned case.

Our experiment demonstrates the richness of the coherent interplay between the molecular orbital, the electron produced by tunnelling, and the emitted photon. Until now, attosecond science has concentrated on controlling the continuum electron [22–25], largely ignoring the other opportunities. Molecules provide another route. Small molecules can match the size and structure of the incoming electron wave better than atoms at XUV wavelength. Therefore, they allow a stronger dipole at the same ionization level. Thus, stronger harmonic and attosecond sources will become available from molecules than from atoms at some wavelengths. Controlling molecular alignment controls the high order nonlinearity—both its amplitude and phase. This opens many new opportunities for quasi-phase-matching, for polarization control, and for attosecond pulse shaping. Further control of high harmonics is possible by molecular orientation [26] leading to the breaking of inversion symmetry. Then even order harmonics can be produced.

Control of harmonics and probing molecular properties are two sides of the same coin. Harmonics provide a very sensitive probe of molecular wave packets. These wave packets can be rotational wave packets as we have demonstrated or they can be vibrational wave packets as might be generated in a photochemical reaction [27]. Equally they can be attosecond electronic wave packets [5]. Harmonics can be used to measure wave packets, and wave packets can be used to control harmonics.

In addition to NRC, the authors acknowledge financial support from the National Science and Engineering Research Council, Photonic Research Ontario, Canadian Institute for Photonic Innovation, and the Alexander von Humboldt-Stiftung.

*Present address: Lawrence Berkeley National Laboratory, 1 Cyclotron Road, Berkeley, CA 94720, USA.
Electronic address: jitatani@lbl.gov

[1] P. B. Corkum, Phys. Rev. Lett. **71**, 1994 (1993).
[2] T. Zuo, A. D. Bandrauk, and P. B. Corkum, Chem. Phys. Lett. **259**, 313 (1996).
[3] H. Niikura *et al.*, Nature (London) **417**, 917, (2002).
[4] M. Lein *et al.*, Phys. Rev. A **66**, 023805 (2002).
[5] J. Itatani *et al.*, Nature (London) **432**, 867 (2004).
[6] Y. Liang *et al.*, J. Phys. B **27**, 5119 (1994).
[7] H. Sakai and K. Miyazaki, Appl. Phys. B **61**, 493 (1995).
[8] B. Shan, S. Ghimire, and Z. Chang, Phys. Rev. A **69**, 021404(R) (2004).
[9] H. Stapelfeldt and T. Seideman, Rev. Mod. Phys. **75**, 543 (2003).
[10] P. W. Dooley *et al.*, Phys. Rev. A. **68**, 023406 (2003).
[11] R. Velotta *et al.*, Phys. Rev. Lett. **87**, 183901 (2001).
[12] R. de Nalda *et al.*, Phys. Rev. A **69**, 031804 (R) (2004).
[13] P. B. Corkum *et al.*, postdeadlined paper to the 4th International Conference on Ultrafast Optics, Vienna, Austria, June 29–July 3, 2003 (unpublished); D. Zeidler *et al.*, *Ultrafast Optics IV*, (Springer-Verlag, New York, 2004), p. 247.
[14] M. Kaku, K. Masuda, and K. Miyazaki, Jpn. J. Appl. Phys. **43**, L591 (2004).
[15] The modulation width of harmonic intensities weakly depends on the harmonic orders. The harmonic spectra are thus numerically integrated to show the trends for the plateau and the cutoff regions for Fig. 1.
[16] M. Yu. Ivanov and P. B. Corkum, Phys. Rev. A **48**, 580 (1993).
[17] A. Paul *et al.*, Nature (London) **421**, 51 (2003).
[18] I. V. Litvinyuk *et al.*, Phys. Rev. Lett. **90**, 233003 (2003).
[19] X. M. Tong, Z. X. Zhao, and C. D. Lin, Phys. Rev. A **66**, 033402 (2002).
[20] P. Dietrich, N. H. Burnett, M. Ivanov, and P. B. Corkum, Phys. Rev. A **50**, R3585 (1994).
[21] The harmonic spectra are numerically integrated over the spectrometer's window including the plateau and the cutoff regions (17th–35th) to improve the signal-to-noise ratio.
[22] M. Ivanov, P. B. Corkum, T. Zuo, and A. Bandrauk, Phys. Rev. Lett. **74**, 2933 (1995).
[23] R. Bartels *et al.*, Nature (London) **406**, 164 (2000).
[24] R. Kienberger *et al.*, Nature (London) **427**, 817 (2004).
[25] H. Niikura *et al.*, Nature (London) **421**, 826 (2003).
[26] H. Sakai *et al.*, Phys. Rev. Lett. **90**, 083001 (2003).
[27] A. Zewail, *Femtochemistry: Ultrafast Dynamics of the Chemical Bond* (World Scientific, Singapore, 1994).